Extension of the ($B^2\Sigma_u^+ - X^2\Sigma_g^+$) System of $^{14}N_2^+$ and $^{15}N_2^+$

K. Boudjarane* and Jow-Tsong Shy

Department of Physics, National Tsin Hua University, Hsinchu, Taiwan, 30043, ROC

M. Larzillière

Laboratoire de Physique Atomique et Moléculaire, Université Laval, Sainte-Foy, Québec, GIK 7P4, Canada

Received: January 27, 1997; In Final Form: April 2, 1997[⊗]

The (0,1) band of the $B^2\Sigma_u^+ - X^2\Sigma_g^+$ system of $^{14}N_2^+$ and $^{15}N_2^+$ has been observed using the fast ion beam laser spectroscopy (FIBLAS) technique. In total, 80 rotational lines were identified as belonging to the (0,1) band. These laser-induced fluorescence (LIF) data for the B−X band, combined with the Fourier transform (FT) emission data for the Meinel $A^2\Pi_u - X^2\Sigma_g^+$ system, allow us to remove the strong correlation between the X and B states and thus properly determine uncorrelated values of the molecular constants for the excited B and perturbed A states. Also, the values of equilibrium molecular constants are reevaluated for $^{14}N_2^+$ and $^{15}N_2^+$.

I. Introduction

The first negative system $B^2\Sigma_u^+ - X^2\Sigma_g^+$ of the molecular ion N_2^+, which was observed firstly by Fasbender[1] in the beginning of the century, has remained one of the most extensively studied ions because of its importance in several fields of physics and chemistry.[2−5] Recently, many sub-Doppler techniques using single-mode lasers have been developed to explore new facets of the internal structure of the nitrogen ion[6−8] not accessible in the past by conventional spectroscopy.[9,10] Since the pioneering work of Gottscho and co-workers[11] where the first complete deperturbation of several bands in the first negative system of N_2^+ was done, fast ion beam laser spectroscopy (FIBLAS) has become a very efficient method for measuring high-resolution spectra of molecular ions.

We used this powerful technique (FIBLAS) to record the LIF high-resolution spectrum of the (0,1) band of the B−X system for the two isotopic molecules $^{14}N_2^+$ and $^{15}N_2^+$. These LIF data were combined with the Fourier transform (FT) measurements[12] of the Meinel A−X band system[13] to remove the presence of strong correlation between the spin−rotation parameters (γ', γ'') of the X ground and B excited states in the first negative system B−X and to determine uncorrelated values of the molecular constants and deperturbed parameters for B and A exited states of $^{14}N_2^+$ and $^{15}N_2^+$. Furthermore, we reevaluated the more precise values of the equilibrium molecular constants by least-squares analysis of our two (0,1) and (1,2) bands[14] combined with other high-resolution Meinel A−X bands[12,15−19] for $^{14}N_2^+$ and $^{15}N_2^+$ using Dunham's formula.[20]

II. Experiment

More details about the experimental setup can be found in previous papers[6,10,21] where the ion and light-laser sources employed in coaxial configuration have been described. The experimental setup mainly consists of a radio-frequency source operated at 60 MHz,[22,23] where a mixture of nitrogen and helium gases was introduced to produce the N_2^+ molecular ions. The extracted ion beam of N_2^+ was focused and accelerated to terminal high voltage in the range 5−15 keV. After two mass selections by a series of magnets, the ion beam interacts collinearly with a CW single-mode dye laser (CR 699, Coherent) running with stilbene 3 dye, which was pumped by an Innova, 15 W CW Ar^+ laser. The vacuum in the beam line was maintained by a diffusion pump near the source, a turbomolecular pump in the line, and two cryogenic pumps between the drift-tube region where the ion and laser beams were focused to interact.

The molecular ions were Doppler tuned into resonance with the single-mode laser frequency by the application of a voltage ramp to the drift tube, which is an electrically isolated section of beam line. The fluorescence induced by the laser was detected by a cooled photomultiplier equipped with a narrow-band-pass interference filter in order to suppress the background light arising from scattered laser light, A/D converted, and transferred to an IBM-PC to be counted by a data acquisition system.

III. Rotational Results

In the study of transitions in the B−X system of $^{14}N_2^+$ and $^{15}N_2^+$, a strong correlation exists between the spin−rotation (γ'', γ') constants of the ground and excited electronic states.[11] Only the difference, $\gamma' - \gamma''$, could be evaluated in the B−X transition. However, in the measurements of the Meinel A−X band system any molecular constants of the excited state $^2\Pi$ correlate significantly with the spin−rotation parameter of the ground state, as previously reported.[12,14] Combining our new high-resolution LIF measurements of the first negative B−X system using a fast ion beam with FT emission data obtained in the Meinel A−X system, we can remove the correlation between X and B state parameters and properly determine the uncorrelated values with more precision for the excited B and A state parameters in the B−X system of $^{14}N_2^+$ and $^{15}N_2^+$.

The sub-Doppler LIF spectra of the (0,1) band of the B−X system for $^{14}N_2^+$ and $^{15}N_2^+$ were recorded respectively in the ranges 23 380−23 392 cm^{-1} and 23 452−23 464 cm^{-1} for $1 < N'' < 22$. Each band represents a recording frequency region of about 12 cm^{-1} obtained by successive partial scans. Each scan was recorded with a fixed energy acceleration to a value between 5 and 15 keV and fixed single-mode laser frequency. A linear voltage was applied to the drift tube in the range 0−1000 V to allow the laser beam to coincide with the desired B−X transition (see ref 14 for more details).

Figure 1 shows a comparison between a typical LIF scan for the (0,1) band for $^{14}N_2^+$ and the corresponding FT emission

[⊗] Abstract published in *Advance ACS Abstracts,* July 1, 1997.

S1089-5639(97)00335-6 CCC: $14.00

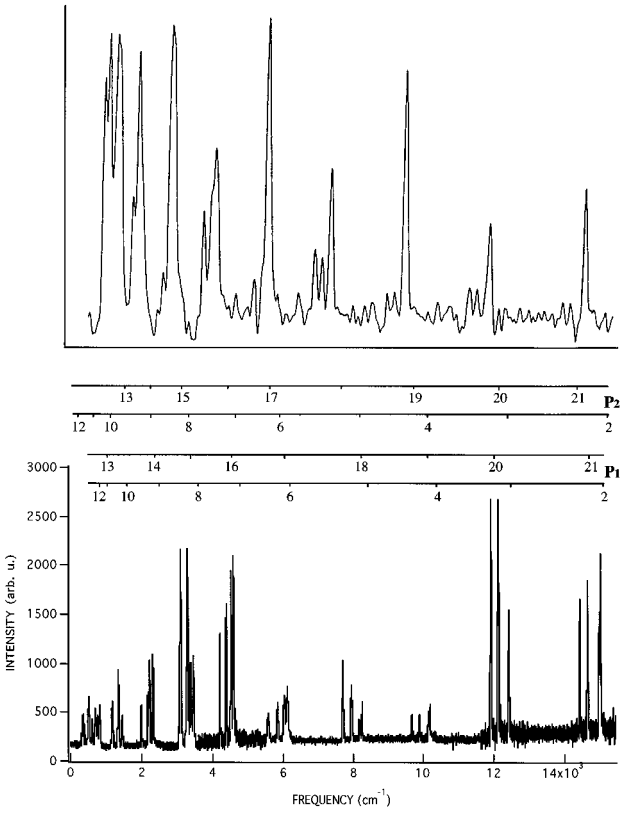

Figure 1. Portion of the LIF spectrum (lower) of the (0,1) band compared to the FT emission spectrum (upper) of the $B^2\Sigma_u^+ - X^2\Sigma_g^+$ transition for the same frequency range.

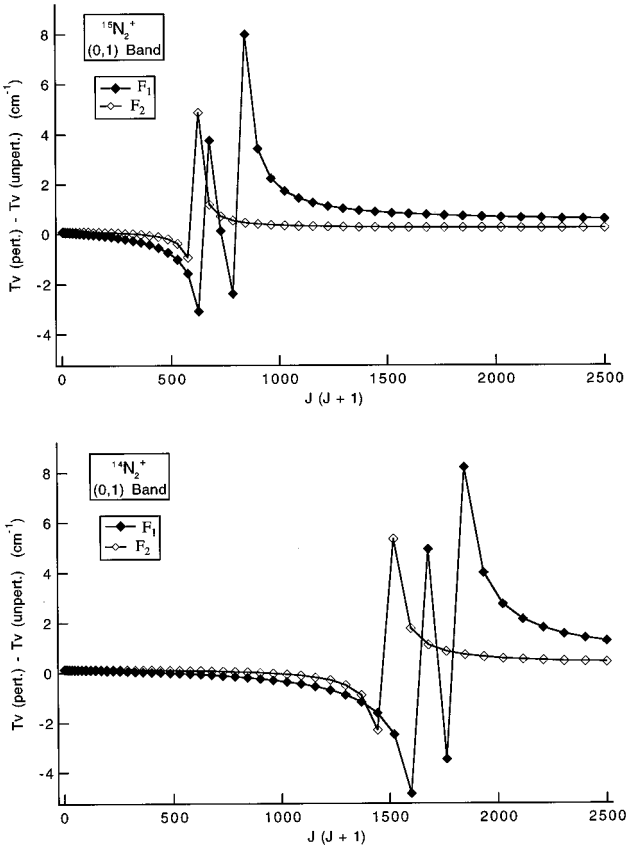

Figure 2. Plot of the difference between the perturbed and unperturbed term values versus $J(J + 1)$ for both spin components F_1 and F_2 of $^{14}N_2^+$ (lower) and $^{15}N_2^+$ (upper). The two spin components are affected by the perturbation for both isotopic molecules.

spectrum recorded for the same frequency range. A difference can be seen between the two spectra in terms of resolution, which has been limited in the FT emission spectrum but improved by the kinematic compression of the velocity distribution in the fast ion beam technique (FIBLAS). This FT emission spectrum was produced in a low-pressure water-cooled discharge lamp by a FT spectrometer, which is calibrated by a frequency-stabilized single-mode He−Ne laser where the absolute precision of a line position is about 0.02 cm^{-1}. This FT emission spectrum and the emission spectral data obtained in ref 8 are used for the calibration of our LIF spectrum of $^{14}N_2^+$. For $^{15}N_2^+$, we used the data of ref 7 to calibrate the line positions against standard iron lines with an accuracy of ±0.002.

The lower part of Figure 1 shows the LIF spectrum of $^{14}N_2^+$ with resolved spin components of the P branch for all the rotational levels. Brons[24] reported the disappearance of spin-doubling for $N < 10$. This discrepancy is related to the lower resolution of his spectra. In addition, the precise and accurate spectra recorded using the FIBLAS technique allowed us to observe the effects of perturbations of the excited B state by the nearby upper A state. In Figure 2, we plotted the difference between perturbed and unperturbed term values versus $J(J + 1)$. This figure clearly shows the effect of perturbation on the rotational lines of both spin components F_1 ($J = N + 1/2$) and F_2 ($J = N - 1/2$) of the (0,1) band in $^{14}N_2^+$ (lower part) and $^{15}N_2^+$ (upper part). We note that this perturbation strongly affects both spin components in $^{14}N_2^+$ and $^{15}N_2^+$, respectively, in the rotational level ranges $N = 35-45$ and $N = 21-31$. Because of the parity dependence of $^2\Sigma^+ - ^2\Pi_{1/2}$ interactions, the effects of perturbation are more important for one parity component because of interference between the spin−orbit and rotation−electronic terms in the effective Hamiltonian.[11,25,26] Thus, the perturbation is larger in the F_1 than the F_2 component, as is shown in Figure 2. This effect was reported in our previous work[14] for the (1,2) band, where the effect of perturbation on the F_2 spin component becomes negligible relative to the other F_1 spin component in the case of $^{14}N_2^+$. However, for $^{15}N_2^+$, both spin components remain unaffected by the perturbation for (1,2) band. This important effect of perturbation of the excited B state by the A state via spin−orbit interactions was observed previously in several experiments, such as those of Brons[24] and Child[27] but with lower precision about the location of the region affected by this perturbation.

The molecular constants and deperturbed parameters of the upper levels were evaluated by using a two-state direct least-squares fit, taking into account the perturbation of the excited electronic $B(v' = 0)$ state arising from rotational levels of the $A(v = 10)$ state. Since both electronic X and B states follow Hund's case (b), these transitions are restricted to $\Delta N = \pm 1$ rotational branches ($\Delta N = 0$ is forbidden for $\Sigma - \Sigma$ transitions). By the spin−rotation interaction, each rotational level splits into two components denoted by F_1 and F_2, respectively, corresponding to $J = N + 1/2$ and $J = N - 1/2$. With high-resolution measurements, we can resolve the spin splitting corresponding to both components for each branch. An analysis of the rotational structure was carried out using standard energy level expressions. For the X state, the Hamiltonian is diagonal in a Hund's case (b) basis with eigenvalues[12]

$$F_1(N) = B_\Sigma N(N+1) - D_\Sigma N^2(N+1)^2 + (1/2)\gamma_\Sigma N \quad (1a)$$

$$F_2(N) = B_\Sigma N(N+1) - D_\Sigma N^2(N+1)^2 - (1/2)\gamma_\Sigma (N+1) \quad (1b)$$

The excited B state was treated in the same way, but including matrix elements with the perturbing A state. The result is a 3

TABLE 1: Rotational Constants (in cm^{-1}) of the $B^2\Sigma_u^+$ ($v' = 0$) and $A^2\Pi_u$ ($v = 10$) States of $^{14}N_2^+$ [a]

constants	present work	previous work (ref 11)
T_Σ	23391.3166(21)	23391.307(10)
B_Σ	2.0745303(70)	2.074555(24)
$D_\Sigma \times 10^5$	0.57000(46)	0.6292(11)
γ_Σ	0.03057(50)	0.0231(10)
T_Π	24227.256(87)	24227.68(10)
B_Π	1.54325(7)	1.54187(11)
A_Π	−74.58 (25)	−74.6[b]
$A_D \times 10^5$	−0.943(57)	
$D_\Pi \times 10^5$	0.600(50)	0.606[b]
ξ	−1.718(5)	−1.747(12)
η	0.13856(6)	0.13912(26)

[a] Numbers in parentheses represent one standard deviation for the last digit. [b] Calculated value (see Table 5 in ref 11).

$\times$ 3 matrix for each J whose elements are[6,19]

$$\langle {}^2\Sigma^{+(e/f)}|H|{}^2\Sigma^{+(e/f)}\rangle = T_\Sigma + B_\Sigma X(X \mp 1) - D_\Sigma X^2(X \mp 1)^2 + (1/2)\gamma(1 \mp X) \quad (2a)$$

$$\langle {}^2\Pi_{1/2}^{(e/f)}|H|{}^2\Pi_{1/2}^{(e/f)}\rangle = T_\Pi + (1/2)A_\Pi + (B_\Pi - (1/2)A_D)X^2 - D_\Pi(X^4 + X^2 - 1) \mp (1/2)(p_v + 2q_v) \quad (2b)$$

$$\langle {}^2\Pi_{3/2}^{(e/f)}|H|{}^2\Pi_{3/2}^{(e/f)}\rangle = T_\Pi + (1/2)A_\Pi + (B_\Pi - (1/2)A_D)(X^2 - 2) - D_\Pi(X^4 - 3X^2 + 3) \quad (2c)$$

$$\langle {}^2\Pi_{3/2}^{(e/f)}|H|{}^2\Pi_{3/2}^{(e/f)}\rangle = -B_\Pi(X^2 - 1)^{1/2} + 2D_\Pi(X^2 - 1)^{3/2} \pm (1/2)q_v X(X^2 - 1)^{1/2} \quad (2d)$$

$$\langle {}^2\Sigma^{+(e/f)}|H|{}^2\Pi_{1/2}^{(e/f)}\rangle = \xi + 2\eta(1 \mp X) \quad (2e)$$

$$\langle {}^2\Sigma^{+(e/f)}|H|{}^2\Pi_{3/2}^{(e/f)}\rangle = -2\eta(X^2 - 1)^{1/2} \quad (2f)$$

where $X = J + 1/2$ and the + and − signs correspond to e and f levels, respectively. The off-diagonal matrix elements in eqs 2e and 2f express the effect of the perturbation and are defined as[11]

$$\xi = \langle v', {}^2\Pi_u|\sum_i \hat{a}_i l_i \cdot s_i|{}^2\Sigma_u^+, v\rangle \quad (3a)$$

and

$$\eta = \langle v', {}^2\Pi_u|BL+|{}^2\Sigma_u^+, v\rangle \quad (3b)$$

and represent the vibronic spin−orbit and vibronic rotation−electronic parameters, respectively. The additional parameters, p_v and q_v, arising from Van Vleck transformations,[25,28] could be important in the treatment of the Meinel A−X band but are relatively small in the B−X system because the contribution of A levels is treated as a perturbation and can be negligible in our fit within our experimental precision.

The molecular constants of the ground X state ($v'' = 1$) were fixed at the uncorrelated values given by Larzilliere et al.[12] in the measurements of the Meinel A−X system for $^{14}N_2^+$. In their work, several bands corresponding to $v'' = 0$, 1, 2 and $v' = 0$, 1, 2, 3 are observed and treated with a resolution of 0.006 cm^{-1} where the molecular constants for the X and A state are derived from the measurements of the emission spectra in the frequency region between 6000 and 13 000 cm^{-1}. All these results, derived from a least-squares fitting procedure of the FIBLAS and the FT data, are listed in Tables 1 and 2, respectively, for $^{14}N_2^+$ and $^{15}N_2^+$.

TABLE 2: Rotational Constants (in cm^{-1}) of the $B^2\Sigma_u^+$ ($v' = 0$) and $A^2\Pi_u$ ($v = 10$) States of $^{15}N_2^+$ [a]

constants	present work	previous work (ref 7)
T_Σ	23460.4092(24)	23460.493(5)
B_Σ	1.937301(19)	1.93731(9)
$D_\Sigma \times 10^5$	0.5573(46)	0.66(2)
γ_Σ	0.02575(95)	0.0011(9)
T_Π	23771.96(21)	23769.40(2)[b]
B_Π	1.4531(77)	
A_Π	−74.454[c]	
$A_D \times 10^5$	0.365(35)	
$D_\Pi \times 10^5$	0.6768(50)	0.6768(59)[b]
ξ	−1.766(79)	−1.7980(9)[b]
η	0.1372(16)	0.13583(2)[b]

[a] Numbers in parentheses represent one standard deviation for the last digit. [b] Reference 29. [c] Calculated value (see ref 11).

Our values of the molecular constants of the excited B state are not in good agreement with the results of Gottscho et al.[11] obtained from measurements of the first negative system (B−X). The value of the spin−rotation parameter (γ') for the excited B state differs by 24% and 15% from ones in refs 11 and 7, respectively, for $^{14}N_2^+$ and $^{15}N_2^+$. Gottscho et al.[11] reported that γ' and γ'' were almost completely correlated with a correlation coefficient of ∼0.95 and so only the difference ($\gamma' - \gamma''$) could be evaluated. Smaller deviations are also observed for the values of the other molecular constants because these constants are also affected by correlation between B and X state parameters. Scholl et al.[29] used a combination of optical and rf data to remove the correlation between the X and B state molecular constants, but the values of the spin−orbit and other molecular constants do not change significantly from those of the previous determination.[11] Probably, with their data set it was not possible to remove the effects of correlation between the ground and the excited state parameters in the first negative system B−X. However, in a A−X transition, the spin−rotation parameter of the ground state does not significantly correlate with any other parameters of the A state as reported by Gottscho et al.[11] and Larzilliere and his co-workers.[12] Hence, the combination of FT data for the Meinel system A−X and FIBLAS data for the B−X transition appears to be the best method to minimize the effects of correlation and to determine the real uncorrelated values of the molecular constants for the excited B and A states, as reported in our previous work.[14]

IV. Vibrational Analysis

The equilibrium molecular constants of the excited B and A states for $^{14}N_2^+$ and $^{15}N_2^+$ can be evaluated using the term value expression introduced by Dunham[20] for a vibrating rotator:

$$E_v = \sum_{ij} Y_{ij}(v + 1/2)^i J^j(J + 1)^j \quad (4)$$

where Y_{ij} represent Dunham's coefficients. However, as reported by Dabrowshi,[30] there is a nonlinear variation of B_v and $\Delta G(v + 1/2)$ at low v, as well as at high v, and the curves cannot be easily described using the power series of expression 4. For that, in practice, it is better to use the following formulas for molecular constants deduced from Dunham's expression 4:

$$B_v = Y_{01} + Y_{11}(v + 1/2) + Y_{21}(v + 1/2)^2 + ... \quad (5a)$$

$$D_v = Y_{02} + Y_{12}(v + 1/2) + ... \quad (5b)$$

To determine these coefficients, the values of our molecular constants for the (0,1) and (1,2) bands[14] were merged in a least-

TABLE 3: Equilibrium Constants (in cm^{-1}) of the $B^2\Sigma_u^+$ State of $^{14}N_2^+$ [a]

constants	present work	previous work (ref 11)
T_e	25460.76171(12)	25461.13(6)
$Y_{10}(\omega_e)$	2422.21798(7)	2420.83(15)
$Y_{20}(-\omega_e x_e)$	−24.62670(11)	−23.85(10)
$Y_{30}(\omega_e y_e)$	−0.21088(51)	−0.359(26)
$Y_{40}(\omega_e z_e)$	−0.0708(70)	−0.0619(20)
$Y_{01}(B_e)$	2.079050(5)	2.08447(15)
$Y_{11}(-\alpha_e)$	−0.016773(15)	−0.02132(13)
$Y_{21}(\gamma_e)$	−0.00157(2)	−0.00085(5)
$Y_{02}(D_e) \times 10^6$	4.713(48)	
$Y_{12}(\beta_e) \times 10^6$	0.43(27)	
r_e (Å)	1.0762589(13)	1.074752
I_e (g cm^2) $\times 10^{39}$	1.3464213	

[a] Numbers in parentheses represent one standard deviation for the last digit.

TABLE 4: Equilibrium constants (in cm^{-1}) of the $A^2\Pi_u$ State of $^{14}N_2^+$ [a]

constants	present work	previous work (ref 12)
T_e	9167.481628(19)	9167.467
$Y_{10}(\omega_e)$	1903.551870(23)	1903.544
$Y_{20}(-\omega_e x_e)$	−15.04753(8)	−15.052
$Y_{30}(\omega_e y_e)$	0.00186(93)	0.00390
$Y_{40}(\omega_e z_e)$		
$Y_{01}(B_e)$	1.7436000(11)	1.74486
$Y_{11}(-\alpha_e)$	−0.0183416(19)	−0.019049
$Y_{21}(\gamma_e) \times 10^{-5}$	−8.09(15)	
$Y_{02}(D_e) \times 10^6$	5.39701(40)	
$Y_{12}(\beta_e) \times 10^6$	0.1151(15)	
A_e	−74.72220(6)	−74.656
α_A	0.05636(13)	0.009
β_A	−0.0054(12)	
r_e (Å)	1.17523799(27)	1.1749
I_e (g cm^2) $\times 10^{39}$	1.60545842	

[a] Numbers in parentheses represent one standard deviation for the last digit.

squares analysis with those of other bands reported in refs 12 and 15−19 and refs 7 and 12 for $^{14}N_2^+$ and $^{15}N_2^+$, respectively. The Y_{i1} and Y_{i2} equilibrium molecular constants in eq 5 were determined from a second-order polynomial in $(v + 1/2)$ and first-order polynomial in $(v + 1/2)$, respectively. However, for the first coefficient Y_{i0} in eq 4, it is better to use the vibrational expression, which can be written as

$$\nu_0 = T_e + \left[\omega'_e\left(v' + \frac{1}{2}\right) - \omega'_e x'_e\left(v' + \frac{1}{2}\right)^2 + ...\right] - \left[\omega'_e\left(v' + \frac{1}{2}\right) - \omega''_e x''_e\left(v' + \frac{1}{2}\right)^2 + ...\right] \quad (6)$$

where the different coefficients for the excited state were determined from fourth-order polynomial in $(v + 1/2)$ by fixing the ones of ground X state parameters to uncorrelated values given in ref 12. For the evaluation of the equilibrium molecular constants corresponding to the A_v parameter, we used the expression

$$A_v = A_e - \alpha_A(v + 1/2) + \beta_A(v + 1/2)^2 \quad (7)$$

The values of the equilibrium molecular constants for the B and A states are listed in Tables 3 and 4 for $^{14}N_2^+$ and in Tables 5 and 6 for $^{15}N_2^+$, respectively. The results of these fits represent the most reliable equilibrium molecular constants for the B and A excited states because of the large amount of high-resolution data used for $^{14}N_2^+$ and $^{15}N_2^+$. These values for the B state (see Table 3 and 5) differ slightly from and are more precise than the previous values for $^{14}N_2^+$ [11,12] and $^{15}N_2^+$,[7,12]

TABLE 5: Equilibrium Constants (in cm^{-1}) of the $B^2\Sigma_u^+$ State of $^{15}N_2^+$ [a]

constants	present work	previous work (ref 7)
T_e	25460.18896(13)	25460.258(9)
$Y_{10}(\omega_e)$	2342.30446(11)	2342.811(9)
$Y_{20}(-\omega_e x_e)$	−24.7041(4)	−24.656(3)
$Y_{30}(\omega_e y_e)$		
$Y_{40}(\omega_e z_e)$		
$Y_{01}(B_e)$	1.947429(11)	1.94775(10)
$Y_{11}(-\alpha_e)$	−0.020139(10)	−0.02046(4)
$Y_{21}(\gamma_e)$	−0.000257(3)	−0.00085(5)
$Y_{02}(D_e) \times 10^6$	4.5097(38)	
$Y_{12}(\beta_e) \times 10^6$	0.1964(93)	
r_e (Å)	1.07432755(26)	1.0742
I_e (g cm^2) $\times 10^{39}$	1.43742127	1.4372

[a] Numbers in parentheses represent one standard deviation for the last digit.

TABLE 6: Equilibrium Constants (in cm^{-1}) of the $A^2\Pi_u$ State of $^{15}N_2^+$ [a]

constants	present work	previous work (ref 12)
T_e	9167.08563(14)	9167.090
$Y_{10}(\omega_e)$	1839.207848(62)	1839.198
$Y_{20}(-\omega_e x_e)$	−14.08440(18)	−14.057
$Y_{30}(\omega_e y_e)$	0.0090(26)	0.00435
$Y_{40}(\omega_e z_e)$		
$Y_{01}(B_e)$	1.6285100(21)	1.628414
$Y_{11}(-\alpha_e)$	−0.0171531(43)	−0.016989
$Y_{21}(\gamma_e) \times 10^{-5}$	−4.26(14)	
$Y_{02}(D_e) \times 10^6$	4.5760(43)	
$Y_{12}(\beta_e) \times 10^6$	0.145(14)	
A_e	−74.65310(11)	−74.657
α_A	0.00598(24)	0.016989
β_A	0.0012(30)	
r_e (Å)	1.17482296(50)	1.1749
I_e (g cm^2) $\times 10^{39}$	1.71891932	

[a] Numbers in parentheses represent one standard deviation for the last digit.

respectively. These discrepancies are related to the remaining correlation between the B and X state parameters in the first negative system B−X transition of Gottscho et al.[11] and Reddy and Prasad.[7] In the case of the perturbed A state (see Table 6), we used the only the third-order polynomial in $(v + 1/2)$ in eq 6 to determine the vibrational constants because of the limited data for the vibrational levels in the range $v = 0-2$. Additional measurements for higher vibrational levels of the first negative B−X and Meinel A−X systems are necessary to have more precise equilibrium molecular constant values for the isotope $^{15}N_2^+$.

V. Isotope Shifts

The observed vibrational isotope shifts were deduced directly from the difference of observed origin bands of $^{14}N_2^+$ and $^{15}N_2^+$, using the expression $\nu_0(^{14}N_2^+) - \nu_0(^{15}N_2^+)$. However, the calculated value can be determined from the vibrational constants and the value of the isotope parameter $\rho = [\mu(^{14}N_2^+)/\mu(^{15}N_2^+)]^{1/2}$ combined with the expression given by Herzberg:[31]

$$\nu_{14} - \nu_{15} = (1 - \rho)[\omega'_e(v' + 1/2) - \omega''_{ee}(v'' + 1/2)] + (1 - \rho)^2[\omega'_e x'_e(v' + 1/2)^2 - \omega''_e x''_e(v'' + 1/2)^2] + (1 - \rho)^3[\omega'_e x'_e(v' + 1/2)^3 - \omega''_e x''_e(v'' + 1/2)^3] + ... \quad (8)$$

The observed and calculated values are listed in Table 7 for the (1,2) and (1,0) bands of the (B−X) system and for the (10,1) band of the (A−X) system. The agreement between the observed and calculated values of isotope shifts is very good and the small difference between them is due to an electronic

TABLE 7: Vibrational Isotopic Shift (in cm^{-1}) of the B−X and A−X Bands System[a]

band	this work	other work	calc[b]
	B−X Band System		
1,2	−60.7092(16)	−61.01[c]	−60.7069
0,1	−69.0926(3)	−69.21[c]	−68.9791
	A−X Band System		
(10,0)	455.36(21)		456.1195

[a] Numbers in parentheses represent one standard deviation for the last digit. [b] Using eq 8. [c] Reference 7.

isotope effect.[31] The comparison of our observed isotope shifts with the results reported earlier[7] gives a difference of 0.30 and 0.12 cm^{-1}, respectively, for the (1,2) and (0,1) bands. This discrepancy is probably due to the effect of perturbations observed in both bands but was not taken into account in the fit by Reddy and Prasad[7] because of their Doppler-limited measurements. Furthermore, we know, in the case of (0,1) band, that both isotopic molecules are affected by the perturbation while just one is affected in the case of the (1,2) band.

The rotational isotope shift is small compared to the vibrational isotope shift but is not negligible. We observed an isotope shift of the rotational constants of 0.134 407(11) and 0.137 229(21) cm^{-1} for $v' = 1$ and $v' = 0$ vibrational levels of the excited B, respectively, while the isotope shift is 0.0902(8) cm^{-1} for the A($v' = 10$) state. A comparison with the calculated values, using the approximate expression 8, gave an insignificant difference, and the very small discrepancy arises from the fact that, in reality, we cannot rigorously separate rotation from vibration when treating the molecule as rovibrating rotator.[31]

VI. Conclusion

Our high-resolution LIF measurements on a fast ion beam of the (0,1) band of the first negative B−X system were combined with the FT emission data to determine uncorrelated values of the molecular constants for the excited B and A states of $^{14}N_2^+$ and $^{15}N_2^+$. The rotational analysis of the (0,1) band was carried out by taking explicitly into account the effects of perturbations of the excited B state by the nearby A state. We have shown the effects of perturbations in both spin components for $^{14}N_2^+$ and $^{15}N_2^+$ of (0,1) but with greater importance for one component. This observation is in good agreement with our previous work[14] for the (1,2) band where the perturbation affects only the F_1 component but appears negligible for the other one in $^{14}N_2^+$. However, any perturbation in both spin components was observed in the case of the $^{15}N_2^+$ isotope for the same band.

We also determined with better accuracy the values of the molecular parameters for the perturbed B state ($v' = 0$) and the perturbing state A($v' = 10$). These new values of deperturbed parameters are more precise than earlier ones[7,11] because we can remove the effects of the strong correlation between the B and X state parameters. Therefore, we have noted a discrepancy between our uncorrelated values for the molecular constants of the excited B and A states and the values reported in earlier studies.[7,11] This reflects the difficulty, as mentioned above, of separating with confidence the individual parameter for the X ground and B excited states where the difference ($\gamma' - \gamma''$) in spin−rotation parameters is much better determined in the experiments on the B−X system.[11,12] Also, we combined our data for the (0,1) and (1,2) bands with other bands of the B−X and A−X systems[11,15−19] in order to determine the equilibrium molecular constants. The results of these fits allow us to present in this work the most reliable values of equilibrium parameters for B and A states of N_2^+. Furthermore, we reported vibrational and rotational isotope shifts between the two isotopic molecules.

Acknowledgment. The financial support of the Canadian National Sciences and Engineering Research Council is gratefully acknowledged. The authors also acknowledge the financial support (Contract No. NSC-85-2-112-M-007-037 and NSC-86-2112-M-007-040) from the National Science Council of Taiwan.

References and Notes

(1) Fasbender, M. *Z. Phys.* **1924**, *30*, 73.
(2) Miller, T.; Bondybey, V. *Molecular Ions: Spectroscopy, Structure, and Chemistry*; North-Holland: New York, 1983.
(3) Vallance, J. A. *Auroral Spectrosc. Space Sci. Rev.* **1971**, 11, 776.
(4) Fauchas, P.; Lapworth, K.; Baronnet, J. *M. First Report on Measurement of Temperature and Concentration of Excited Species in Optically Thin Plasma*; IUPAC Subcommittee on Plasma Chemistry: Limoges, 1978.
(5) McCormac, B. M. *The Radiating Atmosphere Reidel*; Dordrecht: Holland, 1971.
(6) Boudjarane, K.; Lacoursière, J.; Larzillière, M. *J. Chem. Phys.* **1994**, *101*, 10274.
(7) Reddy, S. P.; Prasad, C. V. V. *Astrophys. J.* **1988**, *331*, 572.
(8) Dick, K. A.; Benesch, W.; Crosswhite, H. M.; Tilford, S. G.; Gottscho, R. A.; Field, R. W. *J. Mol. Spectrosc.* **1978**, *69*, 95.
(9) Demtröder, W. *Laser Spectroscopy: Basic Concepts and Instrumentation*; Springer Series in Chemical Physics 5; Springer-Verlag: Berlin, 1981.
(10) Boudjarane, K.; Larzillière, M. *Proc. Int. Conf. Lasers, 17th* **1995**, 520.
(11) Gottscho, R. A.; Field, R. W.; Dick, K. W.; Benesch, W. *J. Mol. Spectrosc.* **1979**, *74*, 435.
(12) Bernard, A.; Larzillière, M.; Effantin, C.; Ross A. G. *Astrophys. J.* **1993**, *413*, 829.
(13) Meinel, A. B. *Astrophys. J.* **1951**, *113*, 583.
(14) Boudjarane, K.; Alikacem, A.; Larzillière, M. *Chem. Phys.* **1996**, *211*, 393.
(15) Harada, K.; Wada, T.; Tanaka, T. *J. Mol. Spectrosc.* **1994**, *163*, 436.
(16) Bachir, H.; Bolvin, H.; Demuynck, C.; Destombes, J. L.; Zellaghi, A. *J. Mol. Spectrosc.* **1994**, *166*, 88; **1995**, *170*, 601.
(17) Ferguson, D. W.; Rao, K. N.; Martin, P. A.; Guelachvili, G. *J. Mol. Spectrosc.* **1992**, *153*, 599.
(18) Cramb, D. T.; Adam, A. G.; Steunenberg, D. M.; Merer, A. J.; Gerry, M. C. L. *J. Mol. Spectrosc.* **1990**, *141*, 289.
(19) Miller, T. A.; Suzuki, T.; Hirota, E. *J. Chem. Phys.* **1984**, *80* (10), 4671.
(20) Dunham, J. L. *Phys. Rev.* **1932**, *41*, 721.
(21) Boudjarane, K.; Carré, M.; Larzillière, M. *Chem. Phys. Lett.* **1995**, *243*, 571.
(22) Larzillière, M.; Jungen, Ch. *Mol. Phys.* **1989**, *67*, 807.
(23) Boudjarane, K. Ph.D. Thesis, Laval University, Québec, Canada, 1992.
(24) Brons, H. H. *Proc., K. Akad. Wet. Amsterdam* **1935**, *38*, 271.
(25) Zare, R. N.; Schmeltekopf, A. L.; Harrop, W. J.; Albritton, D. L. *J. Mol. Spectrosc.* **1973**, *46*, 37.
(26) Hougen, J. I. *The Calculation of Rotational Energy Levels and Rotational Line Intensities in Diatomic Molecules*; NBS Monograph 115; National Bureau of Standards: Washington, DC, 1970.
(27) Childs, W. H. *J. Proc. R. Soc. London, Ser. A* **1932**, *137*, 641.
(28) Van-Vleck, J. H. *J. Chem. Phys.* **1936**, *4*, 327.
(29) Scholl, T. J.; Taylor, A. W.; Holt, R. A.; Rosner, S. D. *J. Mol. Spectrosc.* **1992**, *152*, 398.
(30) Dabrowski, I. *Can. J. Phys.* **1984**, *62*, 1639.
(31) Herzberg, G. *Spectra of Diatomic Molecules*; Van Nostrand: New York, 1950.